Journal of Asian Earth Sciences 40 (2011) 1111–1120

Contents lists available at ScienceDirect

Journal of Asian Earth Sciences

journal homepage: www.elsevier.com/locate/jseaes

Climate and environmental changes during the past millennium in central western Guizhou, China as recorded by Stalagmite ZJD-21

Tz-Shing Kuo [a], Zi-Qi Liu [b], Hong-Chun Li [a,c,*], Nai-Jung Wan [a], Chuan-Chou Shen [d], Teh-Lung Ku [e]

[a] Department of Earth Sciences, National Cheng-Kung University, Tainan 70101, Taiwan, ROC
[b] School of Geographical Sciences, Southwest University of China, Chongqing 400715, China
[c] Department of Geosciences, National Taiwan University, Taipei 10617, Taiwan, ROC
[d] High-precision Mass Spectrometry and Environment Change Laboratory (HISPEC), Department of Geosciences, National Taiwan University, Taipei 10617, Taiwan, ROC
[e] Department of Earth Sciences, University of Southern California, Los Angeles, CA 90089, USA

ARTICLE INFO

Article history:
Available online 19 January 2011

Keywords:
Oxygen and carbon isotopes
Speleothem
Zhijin Cave
Guizhou
Paleoclimate
Karst rocky desertification

ABSTRACT

Stalagmite ZJD-21 (12.3-cm long) was collected from Zhijin Cave in Zhijin County, Guizhou, China. Its ^{210}Pb profile and seven ^{230}Th/^{234}U dates indicate that the stalagmite has grown continuously for the past 1100 years. The δ^{18}O record of ZJD-21 indicates that δ^{18}O in the stalagmite was mainly influenced by rainfall amount and/or summer/winter rain ratio, with lighter values corresponding to wetter climatic conditions and/or more summer monsoonal rains. The ZJD-21 δ^{18}O record suggests: (1) dry/warm climates during AD 950-1100 (overlapping with most of the Medieval Warm Period, MWP, in Europe); (2) strengthening of the summer monsoon from the MWP toward the beginning of the Little Ice Age (LIA) at AD 1250; (3) relatively wet/cold conditions occurred between AD 1250 and 1500, shown by relatively light δ^{18}O values; (4) the summer monsoon intensity strongly declined referred by the increase δ^{18}O trend from AD 1500 to AD 1600, perhaps resulting in dry/cold conditions; and (5) a strongly enhancement of the summer monsoon intensity appeared from AD 1700 to 1950, reflecting wet/cold conditions during the late period of the LIA. On decadal scales the monsoonal climate of central western Guizhou can be either warm/wet and cold/dry, or warm/dry and cold/wet. The δ^{13}C variations in ZJD-21 on decadal-to-centennial scales respond mainly to vegetation changes with heavier values reflecting lesser amount of forest coverage. Prior to AD 1700, the δ^{13}C generally co-varied with δ^{18}O reflecting the expected more extensive vegetation growth (lighter δ^{13}C) under wetter climate (lighter δ^{18}O). However, during the past 300 years the δ^{13}C increased sharply showing an opposite trend to that of δ^{18}O. This observation strongly suggests that a decline of surface vegetation due to an artificial deforestation might have occurred – an occurrence coincident with the large-scale immigration into central western Guizhou in connection with copper-mining activities during the reign of Emperor Yongzheng of Qing Dynasty. Since the late 1890s, especially in the past 50 years, population surge has led to serious karst rocky desertification in the area.

1. Introduction

Karst regions and desert margins are two environments known to represent a fragile ecological system. However, unlike desert margins, the karst landscape is not necessarily the result of harsh climatic conditions. Its ecological fragility mainly stems from the peculiar geological processes involving dissolution of mostly carbonate surface rocks and rapid movement of rainwater through the crevices into the ground (Ford and Williams, 2007). These so-called karst processes conduce to engendering limited amounts of surface water (with relatively high alkalinity), soil development, and vegetation covers (Wang et al., 2004). More importantly, the resulting reduced carrying capacity of the land is vulnerable to further degradation by human activities paying scant attention to judicial land-use planning and practices. Both natural and artificial factors can lead to karst rocky desertification – processes that transform a karst area that was originally covered by vegetation and soil into a rocky, desert-like landscape (Li et al., 2006b; Wang et al., 2004).

Guizhou Province is located near the center of the well-known karst regions of South China. About three quarters of its exposed land are composed of carbonate rocks (Xiong et al., 2002). Although rehabilitation measures have been taken in recent years to promote the sustainability of this fragile geo-ecological environment, karst rocky desertification in the region is much in evidence (Li et al., 2006b). To investigate the causes for this regional

* Corresponding author at: Department of Geosciences, National Taiwan University, Taipei 10617, Taiwan, ROC. Tel.: +886 2 33662929; fax: +886 2 23636095.
E-mail address: hcli1960@ntu.edu.tw (H.-C. Li).

1367-9120/$ - see front matter © 2011 Elsevier Ltd. All rights reserved.
doi:10.1016/j.jseaes.2011.01.001

desertification phenomenon, we set out to reconstruct past, prehistoric climate and vegetation changes of the area, so that the role of natural vs. human culprit to the undesired phenomenon can be better understood. In particular, we aim to understand when the regional desertification took place and how climate changes affected vegetation covers and/or the desertification. Speleothems, i.e., secondary carbonate deposits such as stalagmites and soda-straw stalactites formed in limestone caves, which are abundantly present in Guizhou, afford us the material for the paleo-environmental reconstruction. Their $\delta^{18}O$ and $\delta^{13}C$ compositions contain information on climate and vegetation cover.

Studies carried out during the past decade showed that $\delta^{18}O$ in stalagmites grown in monsoonal areas chiefly reflected monsoonal variability: $\delta^{18}O$ becomes lighter as summer monsoon strengthening which results in increase of either precipitation amount, or monsoonal/non-monsoonal ratio or rainout effect in the upper stream of rainy source, or the combination of the three (Hu et al., 2008; Li et al., 1998b, 2010; Paulsen et al., 2003; Wang et al., 2001, 2005; Yuan et al., 2004). For $\delta^{13}C$ in stalagmites, most studies have pointed to the following governing factors: (1) surface vegetation type, (2) source of soil CO_2, (3) dissolution/precipitation of vadose-zone carbonates, and (4) isotopic fractionation associated with the cave carbonate precipitation involving the kinds of minerals formed, CO_2 degassing, kinetic effects, etc. (Hendy, 1971; Baker et al., 1997; McDermott, 2004; Fairchild et al., 2006). Of these factors, the CO_2 source in soil above a limestone cave exerts the most influence on the $\delta^{13}C$ values in stalagmites and soda-straw stalactites. Many studies have thus used the $\delta^{13}C$ records to decipher vegetation changes attributed to climate and human influences (e.g., Li et al., 1997a,b, 1998a; Bar-Matthews et al., 1999; Genty et al., 2003; Paulsen et al., 2003). The rationale behind such a usage lies in the fact that soil CO_2 derives its carbon isotopic composition from that of soil as well as of the vegetation grown in the soil. More lush vegetation growth under relatively clement climate leads to a higher proportion of organics-derived soil CO_2, hence lighter $\delta^{13}C$. Furthermore, $\delta^{13}C$ of the organics-derived soil CO_2 is affected by the relative abundance of local C_3 and C_4 plants. The C_3 (Calvin-Benson) and C_4 (Hatch-Slack) photosynthetic pathways fractionate carbon isotopes to different extents. The C_3 plants (e.g., trees and most shrubs) flourished under wet/cool climate generally have $\delta^{13}C$ values of −25‰ to −32‰, whereas the more heat- and draught-resistant C_4 plants (e.g., maize, sorghum and prairie grass) have $\delta^{13}C$ values of −10‰ to −14‰ (Cerling et al., 1989; Li et al., 1998a). Based on these considerations, variations of $\delta^{13}C$ in speleothems can be taken to reflect changes in the nature and extent of the vegetation cover with concomitant climate connotations. In general, lighter $\delta^{13}C$ in speleothems connotes cooler/wetter climate conditions (Li et al., 1997a, 1998a; Ku and Li, 1998; Qin et al., 2000).

We report here the study of a stalagmite collected from Zhijin Cave in Zhijin County, Guizhou Province, China. High-resolution time-series stable isotope measurements made on the stalagmite will be compared with the instrumental and historical recordings, as well as the well-dated speleothem $\delta^{18}O$ record in the same region, in an attempt to reconstruct the variations of climate and vegetation cover in central western Guizhou over the last millennium. We will also assess the natural vs. artificial causes for the regional vegetation changes, in hopes of shedding light on the karst rocky desertification issue confronted by the region.

2. Background of the study area and previous studies

Zhijin County (105°20′–106°01′E, 26°21′–26°58′N) is situated in the central western part of Guizhou Province, at the eastern edge of the Yunnan-Guizhou Plateau (Fig. 1). With a hilly topography of karst landscape at an elevation of 1330 m, the region has an annual mean temperature of 15.5 °C and precipitation of 1400 mm. Over 70% of the annual rainfall occurs from May to September, brought in by the East Asian and Indian Summer Monsoons. The explored part of Zhijin Cave has a length of over 12 km, including several large chambers with abundant speleothem deposits that give fame to the cave as one of the most scenic in Asia. Designated since 1982 as a national scenic site, Zhijin Cave and its adjoining area have received due protective measures for conservation. Trees make up most of the vegetation cover. Abundant dripping water and actively-forming cave deposits are found in the cave, which has a yearly uniform temperature of ~15 °C, close to the external annual mean temperature. These observations speak well for the Zhijin Cave deposits as archives of past climate variations.

Guizhou Province has over 5000 karstic caves. Of these, Dongge, Qixing, and Longquan Caves, situated in southeast Guizhou, are but a very few that have been studied for their paleoclimatic records (Zhang et al., 2002, 2003b; Yuan et al., 2004; Wang et al., 2005; Qin et al., 2004; Zhao et al., 2004). Yuan et al. (2004) and Wang et al. (2005) used the Dongge $\delta^{18}O$ record to retrace climate changes over the past 180 ky. By comparing the changes with those derived from Greenland ice cores, deep-sea sediments, and insolation, they concluded that the Dongge record represents a reading of Asian Summer Monsoon strength variations, and that on either long or short timescale, the monsoon strength is steered

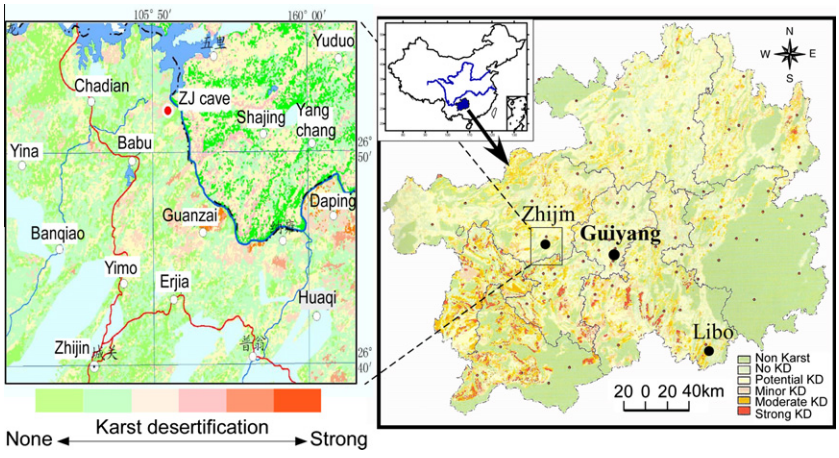

Fig. 1. Location maps of the study area. Map in the right shows Guizhou Province in China and the counties of Zhijin and Libo, where Dongge Cave is located. Map in the left shows the location of Zhijin Cave in Zhijin County. Color codes in the maps indicate the degrees of karst-desertification (Xiong et al., 2002).

mainly by solar insolation, with warm/wet and cold/dry conditions being characteristic of the East Asian Monsoon. Zhang et al. (2002, 2003a) and Qin et al. (2004) studied Qixing Cave in the Duyun region of eastern Guizhou, using isotopic signals as proxy for monsoon variations and discussing Termination II and Heinrich events. Zhao et al. (2004) studied Longquan Cave in the Libo region and reconstructed paleoclimate and paleo-environmental changes during 250–1600 year BP. Based on speleothem $\delta^{18}O$, they placed the Medieval Warm Period – Little Ice Age demarcation at 1600 year BP. The above-cited studies all centered mainly on the application of speleothem $\delta^{18}O$ to climate changes, with relatively little attention paid to local ecosystem changes.

There appears a gap in knowledge concerning environmental changes in terms of climate and ecosystem evolution over the past millennium for the Guizhou area. To begin filling this gap, several recent studies of cave deposits have been carried out to better understand the changes in climate and vegetation cover in central western Guizhou (Li, 2006; Liu, 2008). Isotopic and chemical measurements have also been made on cave dripwater, surface waters and newly formed calcium carbonate deposits from several caves (Zhengjiadong Cave, Shijiangjun Cave and Zhijin Cave) in the Anshun and Zhijin regions (Liu et al., 2007, 2008; Li et al., 2006a). Results indicate that (1) $\delta^{18}O$ and δD values of the regional cave and surface waters fall on the "meteoric water line". The $\delta^{18}O$ of the cave drip water depends on rainfall amount; becoming lighter in the summer rainy season. (2) Isotopic equilibrium exists between the newly formed cave carbonate and cave drip water; cave carbonate deposits may effectively record $\delta^{18}O$ variations of the local meteoric water. (3) Trace element concentrations in cave carbonates may reflect changes in vegetation cover, in addition to be affected by the detrital content and weathering of the host rock. (4) Changes in vegetation cover may also be recorded by changes in $\delta^{13}C$ of cave deposits. The last finding was shown by the $\delta^{13}C$ values of plants, soil organic carbons and modern cave calcite deposits, especially in a ^{210}Pb dated soda-straw stalactite from Zhijin Cave (ZJD-9C) (Liu, 2008). Building upon the foundation provided by these results, the present study on stalagmite ZJD-21 collected in 2007 from Zhijin Cave attempts to reconstruct climate and environmental changes for the past millennium. Emphasis will be placed on examining the humidity/temperature fluctuations on decadal-centennial scales, the regional karst rocky desertification as an evolving process, and the impact of human activities to that process.

3. Sampling and analytical method

The cylindrical stalagmite ZJD-21 is 12.3 cm long with a flat, smooth top (Fig. 2a) that was wet and presumably growing when it was retrieved at about 5 km from the entrance of Zhijin Cave. Split along the growth axis, its translucent section has a fairly uniform appearance in general showing no clearly identifiable laminations and growth hiatus. X-ray diffraction analysis showed that it is composed of calcite.

Powdered samples were drilled from the split section, from locations slightly off-growth axis (see Fig. 2a, between two dotted lines) for ^{210}Pb dating. ^{210}Pb was analyzed via the ^{210}Po alpha-counting method, using a ^{209}Po spike (Li et al., 1996). Polonium was self-plated from an 80 °C solution onto a silver diskette, which was then counted in an ORTEC 576A alpha spectrometric system. The results are given in Table 1 and plotted in Fig. 3.

Samples were also collected along the growth axis for ^{230}Th dating (Fig. 2a) at the High-precision Mass Spectrometry and Environment Change Laboratory (HISPEC) of the National Taiwan University. The sampling locations were selected to generally bracket the upper and lower boundaries of a given zonation showing slight color changes. Analyses of the U and Th isotopes followed the chemistry procedures of Shen et al. (2003). Instrumental analyses were performed using an inductively coupled plasma sector field mass spectrometer (ICP-SF-S) (Shen et al., 2002), Thermo Finnigan Element II, and a multi-collector ICP-MS (MC-ICP-MS) (Frohlich et al., 2009), Neptune. Offline data reduction and calculations of U–Th isotopic compositions and concentrations, and ^{230}Th age were described in Shen et al. (2008). The analytical results and the ^{230}Th dates are shown in Table 2 and Fig. 2b.

For $\delta^{18}O$ and $\delta^{13}C$ analyses, a total of 490 powdered samples were taken along the growth axis (Fig. 2a, between red lines) at an interval of 0.25 mm. Hendy Test (Hendy, 1971) on the stalagmite has proven that the calcite of the stalagmite was deposited under isotopic equilibrium with the cave water. Measurements were done using a Finnigan Delta XP mass spectrometer connected to a Kiel III automatic carbonate-analyzer. The reference gas used was calibrated against the NBS-19 and NBS-18 standards. Analyses of the working standard (NCKU-1) were done after every 5–7 sample measurements to correct for any instrumental drift. Based on the reproducibility of a large number of working standard runs, the analytical errors (one-sigma) were estimated as ±0.11‰ for $\delta^{18}O$ and ±0.05‰ for $\delta^{13}C$. The reported δ values refer to the VPDB standard (at 25 °C). Results are plotted in Fig. 2c.

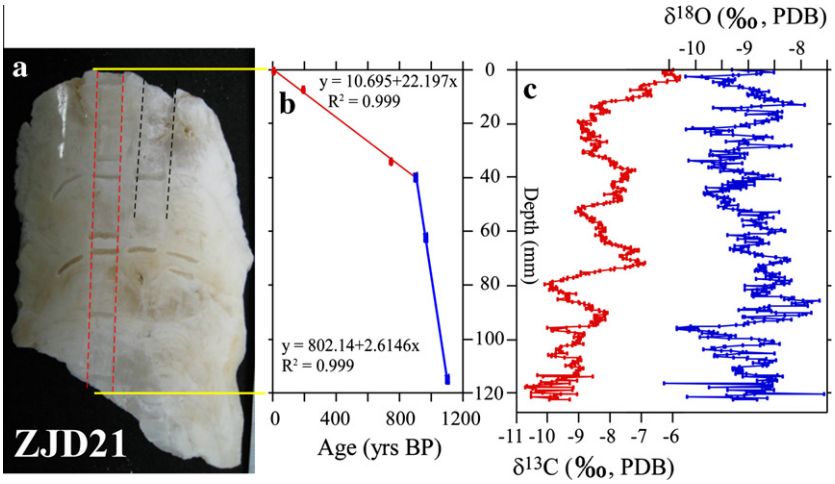

Fig. 2. (a) Photo of stalagmite ZJD-21. The red dashed lines denote the sampling zone for $\delta^{18}O$ and $\delta^{13}C$. The dark dashed lines mark the sampling zone for ^{210}Pb. (b) Age–depth relationship. The ^{230}Th dating results show two distinct growth rates in the stalagmite. (c) The $\delta^{18}O$ and $\delta^{13}C$ records of ZJD-21 (For interpretation of the references to color in this figure legend, the reader is referred to the web version of this article.).

Table 1
^{210}Pb in stalagmite ZJD-21 from Zhijin Cave.[a]

Sample	Distance from tip (cm)	Measured ^{210}Pb (dpm/g)	Excess ^{210}Pb (dpm/g)	Sample	Distance from tip (cm)	Measured ^{210}Pb (dpm/g)	Excess ^{210}Pb (dpm/g)
ZJD-21–0[a]	0.10 ± 0.02	55.2 ± 2.6	55.0	ZJD-21-H	2.75 ± 0.25	2.16 ± 0.24	
ZJD-21-A	0.25 ± 0.25	12.43 ± 0.64	12.29	ZJD-21-J	3.25 ± 0.25	0.006 ± 0.002	
ZJD-21–1[a]	0.40 ± 0.05	10.36 ± 0.61	10.22	ZJD-21-L	3.75 ± 0.25	0.036 ± 0.011	
ZJD-21–2[a]	0.60 ± 0.05	3.09 ± 0.21	2.96	ZJD-21-N	4.25 ± 0.25	0.008 ± 0.003	
ZJD-21-B	0.75 ± 0.25	0.402 ± 0.073	0.265	ZJD-21-P	4.75 ± 0.25	<0.005± < 0.005	
ZJD-21-C	1.25 ± 0.25	0.137 ± 0.037		ZJD-21-R	5.25 ± 0.25	0.013 ± 0.005	
ZJD-21-D	1.75 ± 0.25	0.364 ± 0.080		ZJD-21-T	5.75 ± 0.25	<0.005± < 0.005	
ZJD-21-F	2.25 ± 0.25	1.20 ± 0.17					

[a] Samples were from the second sampling time.

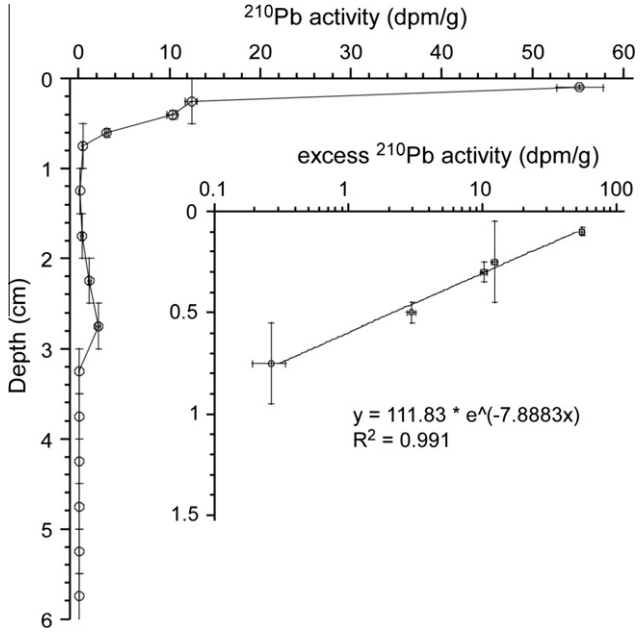

Fig. 3. ^{210}Pb profile of ZJD-21. ^{210}Pb in the upper 0.8 cm exhibits an exponential decrease due to radioactive decay of ^{210}Pb, which indicates an average growth rate of 0.0389 mm/year for ZJD-21.

4. Results and discussions

4.1. Chronology

As shown in Table 1 and Fig. 3, excess ^{210}Pb activities in ZJD-21 are in layers at depths only shallower than ~0.8 cm. Measured ^{210}Pb activities in layers deeper than ~0.8 cm are mostly supported by ^{226}Ra. A semi-logarithmic plot of the ^{210}Pb data shown in Fig. 3 gives an average growth rate of ~0.039 mm/y for the top <8 mm of ZJD-21. If applying the 0.039 mm/y rate to the entire length (123 mm) of the stalagmite, this exercise would give an age of ~3150 year for the bottom layer at 123 mm, which is not supported by the ^{230}Th dating. It suggests that the growth of ZJD-21 has not been uniform in rate.

The very low uranium concentrations of ~0.02 ppm coupled with the young ages of ZJD-21 have posed a considerable challenge to the ^{230}Th dating. These two factors combine to introduce large age uncertainties (Table 2). In spite of the large errors in ages, we may safely conclude from the results that ZJD-21 is younger than 1500 years of age.

The U and Th isotopic data can be treated in another way. Based on the premise that the top layer is modern in age and that no growth hiatus has occurred for the stalagmite, we made an age vs. depth plot as shown in Fig. 2b. In the plot, we opted to eliminate the two data points of ZI2–02 and ZS-04 on account of their large age errors of ±719 years and ±1364 years (Table 2). Two linear segments can be identified in the plot, giving average growth rates of 0.045 mm/y and 0.385 mm/y for the intervals 0–4 cm and 4–12.3 cm, respectively. Fig. 2b shows that growth of ZJD-21 commenced ~1100 years BP and has greatly slowed down since ~800 years BP. The mean growth rate of 0.045 mm/y for the last ~800 years agrees reasonably well with the 0.039 mm/y rate derived from the ^{210}Pb data discussed earlier, considering the age errors involved.

We realize that the ^{230}Th/U chronology of the stalagmite has large uncertainties which do not enable us to compare the ZJD-21 record with other records on annual-to-decadal scales. However, the time-series of the past 800-year record of ZJD-21 is confirmed by both the ^{210}Pb dating and the ^{230}Th/U dates. Thus, it is reasonable to compare this record with other records including historic climate record and speleothem δ^{18}O record in the same region on decadal-to-centennial scales.

Table 2
ICPMS measurements of U and Th isotopes and ^{230}Th/U ages of ZJD-21 samples.[a]

Sample	Depth (mm)	^{238}U ppb	^{232}Th ppt	δ^{234}U meas.	$\left(\frac{^{238}Th}{^{238}U}\right)$	$\left(\frac{^{238}Th}{^{232}Th}\right)$	Age uncorr.	Age corr.	$\delta^{234}U_o$ corr.
Measured by element II ICPMS in 2007									
ZJD-21A	5	22.8 ± 0.1	375 ± 7	685 ± 12	0.0065 ± 0.0056	1.2 ± 1.0	421 ± 365	163 ± 386	685 ± 12
ZJD-21B	70	20.0 ± 0.1	986 ± 9	736 ± 9	0.0164 ± 0.0063	1.02 ± 0.39	1088 ± 365	331 ± 525	736 ± 9
ZJD-21C	115	19.3 ± 0.1	163.0 ± 7.3	739 ± 12	0.0034 ± 0.0065	1.2 ± 2.3	216 ± 406	88 ± 411	739 ± 12
Measured by Neptune ICPMS in 2008									
ZS-02	34	19.50 ± 0.02	255.0 ± 3.9	700.0 ± 2.1	0.0147 ± 0.0021	3.45 ± 0.49	951 ± 134	748 ± 243	701 ± 2.1
ZI1–02	40	16.90 ± 0.02	134.5 ± 2.8	727.0 ± 2.0	0.0162 ± 0.0026	6.2 ± 1.0	1027 ± 168	905 ± 208	729 ± 2.1
ZS-03	62	21.50 ± 0.02	454.5 ± 3.0	728.6 ± 2.3	0.0203 ± 0.0018	2.94 ± 0.27	1291 ± 118	967 ± 345	731 ± 2.4
ZI2–02	68	18.30 ± 0.02	1593.1 ± 6.8	714.8 ± 2.0	0.0350 ± 0.0022	1.231 ± 0.077	2252 ± 141	904 ± 1364	717 ± 3.4
ZS-04	91	12.00 ± 0.02	528.8 ± 6.2	728.9 ± 2.7	0.0360 ± 0.0037	2.49 ± 0.26	2294 ± 238	1617 ± 719	732 ± 3.1
ZS-05	115	14.30 ± 0.01	61.0 ± 2.8	692.3 ± 2.3	0.0180 ± 0.0031	12.9 ± 2.3	1169 ± 199	1102 ± 210	694 ± 2.1

[a] Analytical errors are 2σ of the mean. Age corrections were calculated using a ^{230}Th/^{232}Th atomic ratio of 4 (±4) ppm, a value close to that of the average crustal material. The ±100% error assigned to this ratio is arbitrary.

4.2. Instrumental and historical records in central western Guizhou

Calibrating a paleo-proxy climate record with instrumentally recorded rainfall and temperature is invaluable. However, such a calibration is often limited by the short duration of the instrumental record. In order to compare the ZJD-21 $\delta^{18}O$ record with meteorological observation, we first noted the similar variation patterns in the post-1970 instrumental records of Zhijin County and Guiyang City. The Guiyang City record began in AD 1920 (Fig. 4). In addition, the historic dryness/wetness (D/W) index of Guiyang that has been calibrated with the modern precipitation record extended back to AD 1471 (Chinese Academy of Meteorological Sciences, 1981; Zhang et al., 2003a). This allows us to discern changes in the moisture condition of the area since AD 1471.

Fig. 4 shows that (1) rainfall in Zhijin is higher than that in Guiyang, and temperature in Zhijin is lower than that in Guiyang, due to the higher elevation of Zhijin though the distance between two places is less than 100 km (see Fig. 1); (2) the 5-year running average trends of the two places are the same, so it is reasonable to use the Guiyang record for comparison with the $\delta^{18}O$ record of ZJD-21; and (3) the instrumental records show cold/wet and warm/dry climatic pattern in most years.

4.3. Physical meanings of the stalagmite $\delta^{18}O$

Throughout the investigation of surface water and cave water in Zhijin area during 2006–2008, we have obtained the $\delta^{18}O$ of cave waters which were not influenced by seasonal effect, ranging from −8.46‰ to −7.55‰ (SMOW) with an average of -7.96 ± 0.33‰ (Liu et al., 2008; Liu, 2008). The dripping water for stalagmite ZJD-21 from Silver Rain Palace in Zhijin Cave has $\delta^{18}O$ values of −8.24‰ (SMOW) in January when the stalagmite was collected and −8.02‰ in September of 2006. It seems that the $\delta^{18}O$ of dripping water at this spot does not change much seasonally. Using the water $\delta^{18}O$ value of −8.2‰ and annual mean surface temperature of 15.5 °C in Zhijin County in 2006, we can calculate the calcite $\delta^{18}O$ value under isotopic equilibrium by the following equation (modified from Friedman and O'Neil, 1977; O'Neil et al., 1977):

$$\partial^{18}O_c\ (\text{PDB}) = 3.945 - 0.232 \times T(^\circ C) + \partial^{18}O_w\ (\text{SMOW})$$

where $\delta^{18}O_c$ is the $\delta^{18}O$ of calcite; $\delta^{18}O_w$ is the $\delta^{18}O$ of parent water, and T is the equilibrium temperature. The calculated $\delta^{18}O_c$ is −7.9‰ (PDB) which is about 1‰ heavier than the $\delta^{18}O$ value of surface sample from ZJD-21. This discrepancy may be caused by the uncertainty of water $\delta^{18}O$. Based on the data from Global Network of Isotopes in Precipitation (IAEA/WMO, 2001), the annual weighted $\delta^{18}O$ in precipitation at Zunyi and Guiyang during 1986–1992 vary about 3‰ (Table 3). It is difficult to match the surface sample of ZJD-21 with the water $\delta^{18}O$ in the same year due to slow growth rate and sampling limit. Nevertheless, in previous study, we had demonstrated that the modern calcite deposits in Zhijin Cave are under isotopic equilibrium (Liu et al., 2007), which has been proven by Hendy Test too.

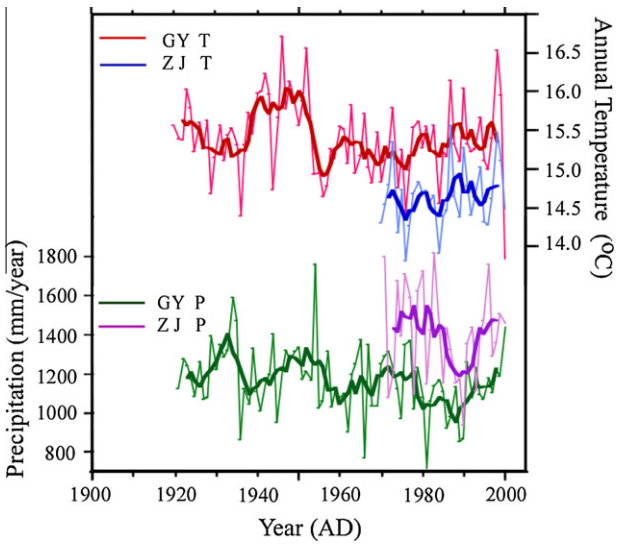

Fig. 4. Instrumental records of Zhijin and Guiyang. Thin lines are annual data, whereas thick lines are 5-year running averages. (See text for discussion.)

Nevertheless, the stalagmite $\delta^{18}O$ records changes in the $\delta^{18}O$ of cave water or annual weighted $\delta^{18}O$ of precipitation above the cave. As mentioned before, stalagmite $\delta^{18}O$ in monsoonal regions chiefly reflected monsoonal variability with lighter values indicating strengthening of the summer monsoon which may result in increase of either precipitation amount, or monsoonal/non-monsoonal ratio or rainout effect in the upper stream of rainy source, or the combination of the three (Hu et al., 2008; Li et al., 2011; Wan et al., 2011; Paulsen et al., 2003; Wang et al., 2001, 2005). Although it is difficult to obtain direct evidence of rainout effect in the upper stream of moisture pathway, the influences of precipitation amount and monsoonal/non-monsoonal rain ratio can be discussed by the monitoring data listed in Table 3. Precipitation $\delta^{18}O$ in central western Guizhou was relatively light in year 1988, 1989 and 1991, and relatively heavy in year 1986–1987 and 1992. The rainfall and summer/winter precipitation ratio in 1988–1989 and 1991 were relatively high, whereas rainfall and summer/winter precipitation ratio in 1990 was certainly low (Table 3). It is difficult to see clearly that the influence of differentiation between Indian monsoon and Western north Pacific monsoon on the precipitation $\delta^{18}O$. Therefore, we conclude that the stalagmite $\delta^{18}O$ of ZJD-21 is mainly an indicator of rainfall amount and summer/winter precipitation ratio in the cave locality, with lighter $\delta^{18}O$ value reflecting more rainfall and summer monsoonal rain; and vice versa.

4.4. Comparison of $\delta^{18}O$ records: ZJD-21 vs. stalagmite DA from Dongge Cave

The detailed $\delta^{18}O$ record of stalagmite DA from Dongge Cave (Wang et al., 2005), with its precise chronological control, affords us the opportunity to cross-check the ZJD-21 data. Located in the Libo County, Dongge Cave is about 240 km southeast of Zhijin Cave (Fig. 1). There is a difference of 2° in latitude and 1000 m in elevation, with Zhijin Cave being higher in both cases.

Fig. 5 shows $\delta^{18}O$ records obtained from the two caves for the last 1200 years. Since these records should mainly reflect the variability of $\delta^{18}O$ in precipitation, some resemblance between them is anticipated, particularly if one allows for the relative inaccuracy in age of ZJD-21 and for comparisons to be made on relatively coarse time resolution. Such a resemblance does show up on time scales longer than 50-year. In particular, the long-term trends for the past 300 years show parallelism, serving to validate the developed ZJD-21 chronology.

The $\delta^{18}O$ in ZJD-21 averages −9.06‰ and fluctuates with amplitude of ~3‰, corresponding to −7.41‰ and ~1‰, respectively, in Dongge Cave DA record. Given the relatively high latitude/elevation of the Zhijin Cave locality and that the moisture-bearing airmass comes from the ocean, the lighter $\delta^{18}O$ values for ZJD-21 appear reasonable.

It should be noted that on decadal or shorter scales, discrepancies between the two records are not unexpected. The two locations differ in elevation by 1 km and are 260 km apart, enough to allow short-term differences in rainfall patterns. In addition, comparison of the two records on decadal scales can be affected by the age uncertainties associated with the Zhijin Cave dataset.

Table 3
Annual precipitation, temperature, weighted $\delta^{18}O$ and δD, monsoonal/non-monsoonal rain ratio, Indian summer monsoon (ISM) index and West northern Pacific monsoon index (Data source: weather and isotopic values are from IAEA/WMO (2001); monsoon index data are from Wang (2006).).

Year	Annual P (mm)	Annual T (°C)	Annual weighted ave. $\delta^{18}O$ (SMOW)	Annual weighted ave. δD (SMOW)	MR/NMR	ISM index (JJAS)	WNPM index (JJAS)
Station 5771300, Zunyi, Guizhou; 27.7°N, 106.88°E; Altitude: 844 m a.s.l.							
1986	800	15.2	−6.79	−44.94	3.8	−0.511	1.246
1987	1059	15.8	−7.15	−47.52	4.4	−2.381	−0.410
1988	930	15.4	−9.13	−61.26	3.8	0.633	−2.163
1989	1152	14.9	−9.05	−60.49	3.8	−0.165	−0.052
1990	791	16.0	−8.72	−47.96	1.9	0.196	1.462
1991	1137	15.4	−9.14	−60.29	5.7	0.018	0.477
1992						0.349	−0.019
Station 5781600, Guiyang, Guizhou; 26.35°N, 106.43°E; Altitude: 1071 m a.s.l.							
1988	837	16.4	−9.08	−57.61	4.1		
1989	1148	14.5	−9.56	−63.34	4.1		
1990	745	16.0	−7.93	−49.84	1.8		
1991	1029	15.5	−8.75	−54.61	4.9		
1992	1043	14.0	−6.23	−35.00	2.7		

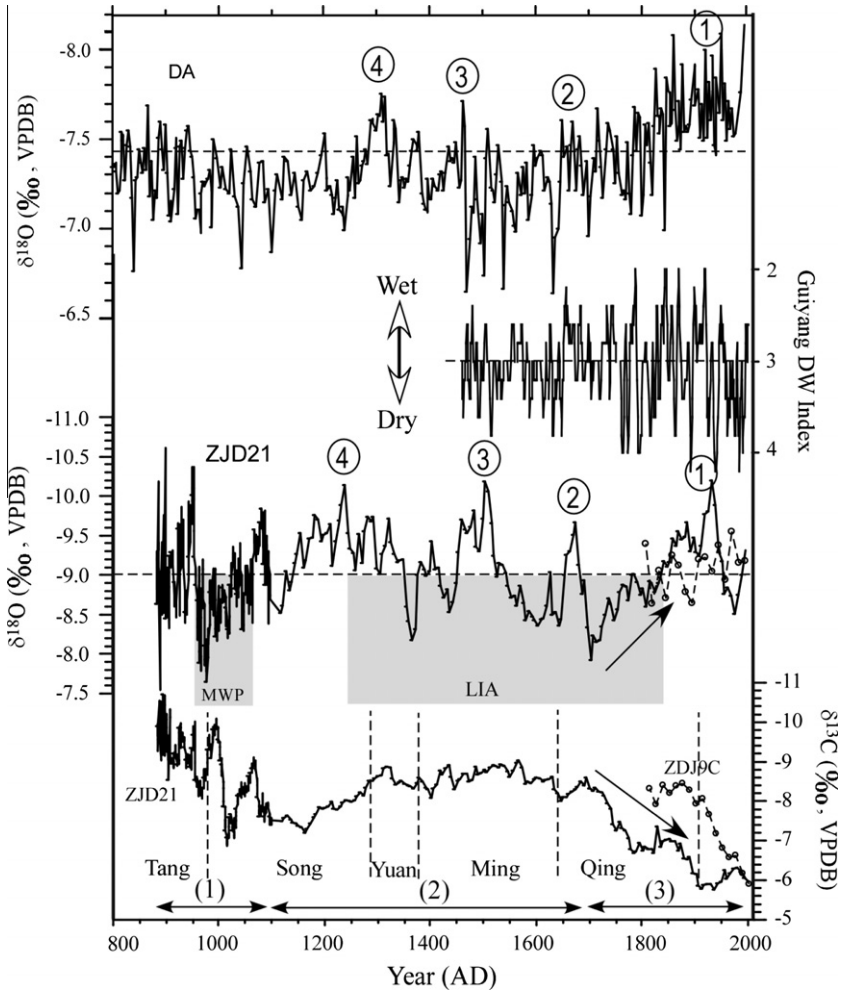

Fig. 5. Comparison of ZJD-21 $\delta^{18}O$ and $\delta^{13}C$ records with the well ^{230}Th-dated DA $\delta^{18}O$ record of Dongge Cave (Wang et al., 2005), the historic D/W index of Guiyang. Horizontal dashed lines denote the average values of each record in the period. The circles with number indicate possible correlations between the ZJD-21 $\delta^{18}O$ record and the DA $\delta^{18}O$ record. The dashed curves with open circles are the $\delta^{18}O$ and $\delta^{13}C$ of soda-straw stalactite ZJD-9C. The shaded areas with MWP, Early LIA and Late LIA denote Medieval Warm Period, early and late Little Ice Age, respectively. Also shown in the figure are three intervals in the ZJD-21 $\delta^{13}C$ record, denoted by the horizontal double-head arrows, marking vegetation changes above the cave. The vertical dashed lines indicate boundaries of Chinese dynasties from Tang to Qing.

4.5. Comparison of $\delta^{18}O$ and $\delta^{13}C$ between ZJD-21 and ZJD-9C

Although no other stalagmite records in central western Guizhou covering the same time interval of ZJD-21 are available up-to-date, a soda-straw stalactite, ZJD-9C, collected from Zhijin Cave in 2006 provides a comparison of the isotopic records within the last 200 years. The 8-cm long ZJD-9C was subsampled at 0.5 cm interval. The 16 subsamples show excellent ^{210}Pb decay trend

which yield a linear growth rate of 0.408 ± 0.0165 cm/y since AD 1810 assuming the stalactite was continuously growing until 2006 (Liu, 2008). The $\delta^{18}O$ and $\delta^{13}C$ of ZJD-9C are plotted with ZJD-21 in Fig. 5. For $\delta^{18}O$, ZJD-21 and ZJD-9C have similar variation ranges and mean values. Age uncertainty and different data resolution between the records make difficulty to match the curves. For $\delta^{13}C$, the two records have similar trends though the $\delta^{13}C$ values of ZJD-9C are heavier. It is clear that speleothem $\delta^{13}C$ at different dripping site in the same cave can be very different (Baker et al., 1997). However, the $\delta^{13}C$ trend may reflect vegetation change above the cave. In addition, seven modern cave calcite deposits (tip of soda-straw ZJD-9A, -9B, -9C, -11A, -17, -25 and deposit on a light bulb ZJD-15) have $\delta^{13}C$ values ranging from −7.06‰ to −5.35‰ with an average of −5.96 ± 0.61‰ (Liu, 2008). This average value is very close to the $\delta^{13}C$ value of the ZJD-21 surface layer that is −5.99‰. The similarity of the ZJD-21 and ZJD-9C $\delta^{13}C$ trends encourage us to interpret the $\delta^{13}C$ records as an indicator of vegetation change in our study.

4.6. Climate variations in central western Guizhou over the past 1100 years

Based on the Fig. 2b chronology, the time variations of $\delta^{18}O$ and $\delta^{13}C$ of ZJD-21 are plotted in Fig. 5, together with the historical Guiyang D/W record (Chinese Academy of Meteorological Sciences, 1981; Zhang et al., 2003a). A correlation between wet climate and light $\delta^{18}O$ on the 10–100-year scale is shown during the past 400 years (Fig. 5). Note that the hollow double arrows in the figure denote the dry climate-heavy $\delta^{18}O$ correlation. These correlations reinforce the usage of $\delta^{18}O$ as a D/W proxy.

$\delta^{18}O$ values in ZJD-21 range from −10.6‰ to −7.6‰ and mean value is −9.06‰ (Fig. 5). Since the chronology of the ZJD-21 has large uncertainty, it is not realistic to the interpret climate change on annual-to-decadal scales. In Fig. 5, the $\delta^{18}O$ of ZJD-21 was relatively heavy during the AD 900–1100 within the Medieval Warm Period (MWP). Around AD 980, the $\delta^{18}O$ reached its heaviest value at −7.6‰. The DA $\delta^{18}O$ record also shows relatively heavier values than its mean $\delta^{18}O$ for the same period, indicating relatively weak summer monsoon during MWP. Thus, climate in central western Guizhou during the Medieval Warm Period can be characterized as warm/dry. From MWP toward the beginning of the Little Ice Age (LIA) at AD1250, the $\delta^{18}O$ of ZJD-21 had a decreasing trend with about 2‰ change, reflecting the summer monsoon strengthening (Fig. 5). Between AD 1250 and AD 1500, the $\delta^{18}O$ values were relatively light, except two heavy $\delta^{18}O$ swings around AD 1400 and AD 1450. From AD 1500 to AD 1600, the elevated $\delta^{18}O$ indicated weakening of the summer monsoon. The DA $\delta^{18}O$ record also exhibited heaviest value in this interval. Therefore, a cold/dry climatic condition was prevailing during this period. A light $\delta^{18}O$ swing existed around AD 1650, reflecting climate returned wet condition in this short interval. From AD 1700 to AD 1950, both ZJD-21 and DA records showed strong $\delta^{18}O$ decrease, from −8‰ to −10.5‰ in the ZJD record. This strong decrease in the $\delta^{18}O$ indicates that the summer monsoon intensity had been enhanced during the late period of the LIA (Fig. 5). After 1950, the summer monsoon declined shown by increased $\delta^{18}O$. Previous works held that monsoon climates have only two major modes: warm/wet and cold/dry (Wang et al., 2001, 2005; Yuan et al., 2004). This thinking may be correct for orbital (i.e., glacial/interglacial) time scales. But for short scales (i.e., decadal to centennial) the monsoonal climate may further include the warm/dry and cold/wet modes. Furthermore, according to modern meteorological data, strong summer monsoon in eastern China does not necessarily bring about enhanced precipitation in Guizhou area. It may bring about reduced precipitation at Dongge Cave region in southeastern Guizhou (Guo et al., 2003; Zhang et al., 2010).

4.7. Changes in vegetation cover at/near Zhijin Cave over the past 1100 years and influence by human activities

The ZJD-21 $\delta^{13}C$ record has trended towards heavier values from AD 900 (–10.6‰) to the present (–6‰) (Fig. 5). The record displays three intervals with different trending patterns: (I) AD 900–1100, varying between –10.6‰ and –7‰ with relatively large fluctuations; (II) AD 1100–1700, varying between –9‰ and –7‰ with relatively small fluctuations; (III) since AD 1700, increasing from –8.5‰ to –6‰ with little fluctuations.

Between AD 880 and AD 980 in Interval I, $\delta^{13}C$ had a similar pattern as $\delta^{18}O$, indicating that climate was the primary factor affecting surface vegetation; human intervention was minimal (Fig. 6). As climate turned wetter, vegetation flourished, producing more soil CO_2 from decomposition of organic matter so as to lower the stalagmite $\delta^{13}C$ down the geochemical pathway. There should be a 10–20 years delay between the $\delta^{18}O$ (rainfall) and $\delta^{13}C$ (vegetation) signals (Ku and Li, 1998). It should be noted that prior to the first wave of immigration to central western Guizhou occurring around early Song Dynasty ca. AD 960 and later (Ge, 2005), the region was thinly populated with its vegetated land minimally disturbed by human activities. In Fig. 6, two strong $\delta^{13}C$ increases occurred from AD 1005 to AD 1015 and from AD 1070 to AD 1075, perhaps reflecting human activity during the early settlements in the Zhijin Cave area. These two $\delta^{13}C$ shifts are difficult

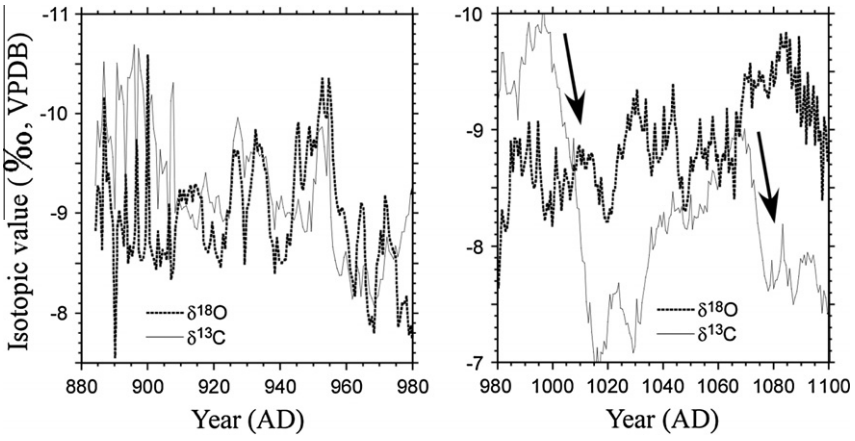

Fig. 6. The $\delta^{18}O$ and $\delta^{13}C$ records of ZJD-21 during AD 880–1100. The high-resolution records show that $\delta^{18}O$ and $\delta^{13}C$ were generally in phase between AD 880 and AD 980, reflecting climatic control on vegetation. Two strong increases in the $\delta^{13}C$ around AD 1000 and AD 1070 might be partially attributed to human activity.

to explain by climate reason. While the above hypothesis needs more evidence to support, our records provide a pilot study on the speleothem $\delta^{13}C$ as a useful tool for reconstruction of paleovegetation change.

During interval II, $\delta^{13}C$ remained relatively stable. As the climate turned wetter, $\delta^{13}C$ decreased from –7.8‰ at AD 1100 to –8.8‰ at AD 1320. In the ensuing 300 years, the variations were less than 1‰. The mean $\delta^{13}C$ is heavier than that of interval I. The difference may be attributable to the reduction of vegetation cover and its C_3/C_4 plant ratio. Since interval II, the stalagmite has grown much more slowly than before. The slower growth rate might be attributed to the reduction of vegetation cover as reduced organic decomposition would lead to lower CO_2 concentrations in soil. As a consequence of the slower growth rate, carbonate precipitation took longer time, so that CO_2 in the cave water would enhance isotopic exchange with the cave atmospheric CO_2, which normally has a heavier $\delta^{13}C$ value than that of dissolved inorganic carbon (DIC) in cavewater. The three factors including decrease in organic carbon, decrease in C_3/C_4 plant ratio, and CO_2 exchange all could lead to enrichment of $\delta^{13}C$ in the stalagmite.

During the last 300 years, i.e., interval III, variations of $\delta^{18}O$ and $\delta^{13}C$ assumed opposite trends (Fig. 5). $\delta^{18}O$ gradually became lighter by more than 2‰ from AD 1700 to AD 1950, suggesting a gradual increase of rainfall. In contrast, $\delta^{13}C$ became heavier in the same period, pointing to human activities rather than climate, which had negative impact on forest growth. The growth rate during interval III was similar to that during interval II. The heavier $\delta^{13}C$ values during interval III than during interval II cannot be explained by growth rate. Deforestation seems the only reason for the increase of $\delta^{13}C$.

Han (2006) pointed out that desertification in certain parts of Guizhou through military encampment and land cultivation may be traced back to the time of Ming Dynasty. Large-scale development of the area, however, began in earnest under the reign of Emperor Yongzheng (AD 1722–1735) of Qing Dynasty (Liang, 1980). Mining activities in western and southern Guizhou added to the population surge (Han, 2006). As a result, the fragile karst environment and its ecosystem were under unprecedented stress. Statistical summaries of the population and farmland developmental history of Guizhou and China are given in Tables 4 and 5, which should serve as a useful base for examining the human impact on environments.

Fig. 7 shows the upward swing of population density increase in both China and Guizhou since the Yongzheng time. Guizhou's population density greatly increased until late in the rule of Emperor Qianlong (AD 1724–1788) before leveling out. The 64% increase from AD 1714 to AD 1751 in Guizhou (Table 4) was riding on mining activities. Accompanying the population surge was the rapid expansion of farmland, which out-paced that of China as a country (Table 5 and Fig. 7).

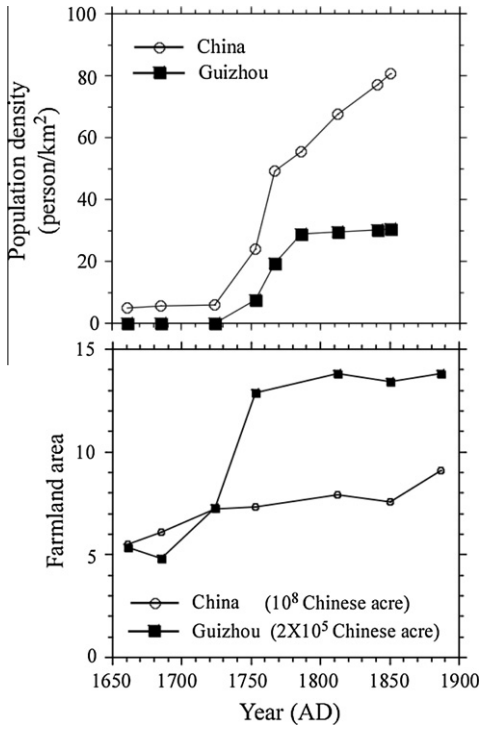

Fig. 7. Changes in population densities (upper panel) and areas of farmland (lower panel) in China and Guizhou during Qing Dynasty (Data from Liang, 1980). From AD 1724 to 1786 the population density in Guizhou had large increases; a 64-fold increase occurred from 1724 to 1753. From AD 1685 to 1753 the farmland area in Guizhou had the largest increases.

Table 4
Changes in population density of China and Guizhou Province during the Qing Dynasty.[a]

Dynasty year	Shunzhi 18th year	Kangxi 24th year	Yongzheng 2nd year	Qianlong 18th year	Qianlong 32nd year	Qianlong 53rd year	Jiaqing 17th year	Daoguang 20th year	Xianfeng 1st year
Calendar year	1661	1685	1724	1753	1767	1788	1812	1840	1850
Density in China (person/km^2)	4.93	5.48	5.92	24.06	49.14	55.49	67.57	77.01	80.69
Density in Guizhou (person/km^2)	0.08	0.08	0.12	7.69	19.31	29.00	29.68	30.32	30.5
Change in China (%)	–	0.11	0.08	3.06	1.04	0.13	0.22	0.14	0.05
Change in Guizhou (%)	–	0	0.5	63.08	1.51	0.5	0.02	0.02	0.01

[a] The changing rate is calculated by using the relationship: (number in year 2 – number in year 1)/number in year 1. (Data from Liang (1980).)

Table 5
Changes in Farmland area of China and Guizhou Province during the Qing Dynasty.[a]

Dynasty year	Shunzhi 18th year	Kangxi 24th year	Yongzheng 2nd year	Qianlong 18th year	Jiaqing 17th year	Xianfeng 1st year	Guangxu 13th year
Calendar year	1661	1685	1724	1753	1812	1850	1887
Area in whole China (10^8 Chinese acre)	5.49	6.08	7.24	7.35	7.92	7.56	9.12
Area in Guizhou (2×10^5 Chinese acre)	5.37	4.8	7.27	12.87	13.83	13.43	13.83
Guizhou/China ratio (%)	0.196	0.158	0.201	0.35	0.349	0.355	0.303
Change in China (%)	–	10.65	19.05	1.6	7.66	−4.44	20.57
Change in Guizhou (%)	–	−10.67	51.56	76.93	7.48	−2.91	2.96

[a] The changing rate is calculated by using the relationship: (number in year 2 – number in year 1) * 100/number in year 1. (Data from Liang (1980).)

The extent and rapidity of the population and land-use increase provided the prescription for environmental deterioration, its manifestation being the karst rocky desertification in parts of Guizhou. Historical records have documented that development of Guizhou peaked at the Yongzheng ~ early Qianlong period of AD 1724–1753. This period also marked the beginning of increasing $\delta^{13}C$ as registered by stalagmite ZJD-21 in Zhijin Cave. Thus one sees the following linkage for an ecologically fragile karst environment: immigration/settlement – farmland expansion – deforestation – rocky desertification – $\delta^{13}C$ in cave deposit turning heavier. For the past 50 years, greatly expanded land development and population in Guizhou (which has a tenfold increase over that during the Qing Dynasty) have altered the landscape to the point that one would hardly expect its modern cave deposits to register $\delta^{13}C$ signals reflecting the pre-development environment.

5. Conclusions

An analysis of the $\delta^{18}O$ and $\delta^{13}C$ records of stalagmite ZJD-21 from Zhijin Cave has led to the following conclusions:

(1) A comparison with instrumental and historical records shows that $\delta^{18}O$ in stalagmite ZJD-21 from Zhijin Cave mainly reflect local rainfall amount variations and changes in monsoonal/non-monsoonal rain ratio, e.g., wetter climate with more summer monsoonal rain gives rise to lighter $\delta^{18}O$.
(2) There is a resemblance between the ZJD-21 and DA (Dongge Cave) $\delta^{18}O$ records on 10–100-year time scale, showing stalagmite $\delta^{18}O$ as proxy for variations in regional climate. In the Zhijin region, strengthening of the summer monsoon and relatively wet climate prevailed during AD 1250–1500 and 1700–1950, while weakening of the summer monsoon and relatively dry conditions prevailed during AD 950–1100 and 1500–1600. On short time scale of 10–100-years, monsoon climate exhibits all combinations of warm/wet, cold/dry, warm/dry and cold/wet conditions. Climate in the Zhijin area exhibited mainly cold/wet during the late period of Little Ice Age. Dry climate prevailed during the Medieval Warm Period at Zhijin.
(3) $\delta^{13}C$ in ZJD-21 reflects variations in the extent of vegetation cover above the cave. The more extensive the vegetation cover, the lighter the $\delta^{13}C$. Prior to the South Song Dynasty, lack of human influence on local vegetation rendered the $\delta^{18}O$ and $\delta^{13}C$ variations similar. Increasing human activities have reduced the vegetated land area and its C_3/C_4 plant ratio, rendering the stalagmite $\delta^{13}C$ heavier.
(4) The $\delta^{18}O$ record of ZJD-21 shows an increase in rainfall over the past 300 years. However, human activities in connection with the surge in population and land use in Guizhou since the Yongzheng era of Qing Dynasty have negatively impacted the local vegetation growth, such that it more than offset the positive impact of rainfall increase. Such an offset has been indicated by the $\delta^{13}C$ records in ZJD-21.

Acknowledgments

Funding for this study was provided by the Science Council of Taiwan (NSC 97-2628-M-006-014, 98-2116-M-006-003 and 98-3114-E-006-014), the National Natural Science Foundation of China (Grant No. 40672202) and a special research grant for Academicians from the Chongqing Science and Technology Commission (Grant No. 20037835). Liu ZQ thanks for funding support from The National Key Technology R&D Program (Grant No. 2006BAC01A09) and Doctoral foundation of Southwest University (Grant No. SWUB 2008060). Funding for ^{230}Th dating at the HISPEC was supported by the NSC Grants (98-2116-M-002-012 and 98-2611-M-0092-006 to CCS). We thank two anonymous reviewers for their constructive and useful comments.

References

Baker, A., Ito, E., Smart, P.L., McEwan, R.F., 1997. Elevated and variable values of ^{13}C in speleothems in a British cave system. Chemical Geology 136, 263–270.
Bar-Matthews, M., Ayalon, A., Kaufman, A., Wasserberg, G., 1999. The Eastern Mediterranean paleoclimate as a reflection of regional events: Soreq cave, Israel. Earth and Planetary Science Letters 166, 85–95.
Chinese Academy of Meteorological Sciences, 1981. Yearly Charts of Dryness/Wetness in China for the Last 500-Year Period, Beijing. SinoMap Cartogr. Publ. House, Beijing (in Chinese).
Cerling, T.E., Quade, J., Wang, Y., Bowman, J.R., 1989. Carbon isotopes in soils and paleosoils as ecology and paleoecology indicators. Nature 341, 138–139.
Fairchild, I.J., Smith, C.L., Baker, A., Fuller, L., Spötl, C., Mattey, D., McDermott, F.E.I.M.F, 2006. Modification and preservation of environmental signals in speleothems. Earth-Science Reviews 75, 105–153.
Ford, D.C., Williams, P.W., 2007. Karst Hydrogeology and Geomorphology. John Wiley & Sons, Ltd., England. 562p.
Friedman, I., O'Neil, J.R., 1977. Compilation of stable isotope fractionation factors of geochemical interest. US Geological Survey Professional Paper, P-0440-KK, pp. 1–12.
Frohlich, C., Hornbach, M.J., Taylor, F.W., Shen, C.-C., Moala, A., Morton, A.E., Kruger, J., 2009. Huge erratic boulders in Tonga deposited by a prehistoric tsunami. Geology 37, 131–134.
Ge, J.X., 2005. Population History of China. Fudian University Press, Shanghai, 6 volumes, 3946p (in Chinese).
Genty, D., Blamart, D., Ouahdi, R., Gilmour, M., Baker, A., Jouzel, J., Van-Exter, S., 2003. Precise dating of Dansgaard–Oeschger climate oscillations in western Europe from stalagmite data. Nature 421, 833–837.
Guo, Q.Y., Cai, J.N., Shao, X.M., Sha, W.Y., 2003. Interdecadal variability of East-Asian summer monsoon and its impact on the climate of China. Acta Geographica Sinica 4, 569–576 (in Chinese).
Han, Z.Q., 2006. Exploitation of Guizhou province during the Yongzheng reign-period and its effect on the Rock-Desertification in this area. Fudan Journal (Social Sciences) 2, 120–140 (in Chinese).
Hendy, C.H., 1971. The isotopic geochemistry of speleothems: I. The calculation of the effects of different modes of formation on the isotopic composition of speleothems and their applicability as palaeoclimatic indicators. Geochimica et Cosmochimica Acta 35, 801–824.
Hu, C., Henderson, G.M., Huang, J., Xie, S., Sun, Y., Johnson, K.R., 2008. Quantification of Holocene Asian monsoon rainfall from spatially separated cave records. Earth and Planetary Science Letters 266, 221–232.
IAEA/WMO, 2001. Global Network of Isotopes in Precipitation. The GNIP Database. <http://isohis.iaea.org>.
Ku, T.-L., Li, H.-C., 1998. Speleothems as high-resolution paleoenvironment archives: records from northeastern China. Journal of Earth System Science 107, 321–330.
Li, H.-C., Ku, T.-L., Chen, W.-J., Jiao, W.-Q., Zhao, S.-S., Chen, T.-M., Li, T.-Y., 1996. Isotope studies of Shihua Cave, Beijing – II: radiocarbon dating and age correction of stalagmite. Seismology and Geology 18, 329–338.
Li, H.-C., Ku, T.-L., Chen, W.J., Li, T.Y., 1997a. Isotope studies of Shihua Cave – III: reconstruction of paleoclimate and paleoenvironment of Beijing during the last 3000 years from $\delta^{18}O$ and $\delta^{13}C$ records in stalagmite. Seismology and Geology 19, 77–86 (in Chinese).
Li, H.-C., Ku, T.-L., Stott, L.D., Yuan, D.X., Chen, W.J., Li, T.Y., 1997b. Interannual–resolution $\delta^{13}C$ record of stalagmites as proxy for the changes in precipitation and atmospheric CO_2 in Shihua Cave, Beijing. Carsologica Sinica 16, 285–295 (in Chinese).
Li, H.-C., Ku, T.-L., Chen, W.J., Yuan, D.X., Li, T.Y., 1998a. Applications of high-resolution carbon isotope records of a stalagmite from the Shihua Cave, Beijing – $\delta^{13}C$ record of deforestation after the establishment of the Grand Capital (Yuan Dadu) in 1272 AD. Geological Review 44, 456–463 (in Chinese).
Li, H.-C., Ku, T.L., Stott, L.D., Chen, W.J., 1998b. Applications of interannual-resolution stable isotope records of speleothem: climatic changes in Beijing and Tianjin, China during the past 500 years – the $\delta^{18}O$ record. Science in China 41, 362–368.
Li, H.-C., Lee, Z.-H., Wan, N.-J., Shen, C.-C., Li, T.-Y., Yuan, D.-X., Chen, Y.-H., 2011. Interpretations of $\delta^{18}O$ and $\delta^{13}C$ in aragonite stalagmites from Furong Cave, Chongqing, China: A 2000-year record of monsoonal climate. Journal of Asia Earth Sciences 40, 1121–1130.
Li, J.Y., 2006. The Response to Climate and Environment Change of Trace Element Ratio from Speleothem in Central Western Guizhou, China. M.Sc. Thesis, Southwest University of China, Chongqing, 54p (in Chinese).
Li, J.Y., Li, H.-C., Liu, Z.Q., Yuan, D.X., He, X., Wang, R.M., 2006a. Geochemical features and Mg/Sr ratio of the samples from cave water and speleothem in central western Guizhou, China. Carsologica Sinica 25, 176–186 (in Chinese).
Li, Y.B., Bai, X.Y., Zhou, G.F., Lan, A.J., Long, J., An, Y.L., Mei, Z.M., 2006b. The relationship of land use with karst rocky desertification in a typical karst area, China. Acta Geographica Sinica 61, 624–632 (in Chinese).

Liang, F.Z., 1980. The Statistics of Family Numbers, Farmland Areas, Farm Taxes in Chinese History. Shanghai People Press. p. 272 and p. 380 (in Chinese).
Liu, Z.Q., 2008. Applications of Geochemical Proxies in Speleothem to the Study on Evolution and Impact Factor of Karst-Desertification in Central Western Guizhou During Modern and Contemporary Period. Ph.D. dissertation, Southwest University of China, Chongqing, 114p (in Chinese).
Liu, Z.Q., Li, H.-C., Xu, Z.M., Yuan, D.X., Li, J.Y., Wan, N.J., He, X., 2007. Stable isotopes of water and carbonate samples from caves in central western Guizhou: implications of paleoclimate and paleoenvironment. Geological Review 53, 233–241 (in Chinese).
Liu, Z.Q., Li, H.-C., Xiong, K.N., Yuan, D.X., Ying, B., Xu, X.M., Li, J.Y., 2008. Implication for sampling paleo-climate indicators by monitoring seasonal variations of δD and δ^{18}O in cave waters. Carsologica Sinica 27, 139–144 (in Chinese).
McDermott, F., 2004. Palaeo-climate reconstruction from stable isotope variations in speleothems: a review. Quaternary Science Reviews 23, 901–918.
O'Neil, J.R., Shaw, S.E., Flood, R.H., 1977. Oxygen and hydrogen isotope compositions as indicators of granite gneiss in the New England Botholith, Australia. Contribution to Mineral Petrology 62, 313–328.
Paulsen, D.E., Li, H.-C., Ku, T.-L., 2003. Climate variability in central China over the last 1270 years revealed by high-resolution stalagmite records. Quaternary Science Reviews 22, 691–701.
Qin, J.M., Yuan, D.X., Cheng, H., Lin, Y.S., Zhang, M.L., Wang, H., Feng, Y.M., Tu, L.L., 2004. A high resolution late Pleistocene climato-stratigraphy of 4 stalagmites from Qixing Cave, Duyun, Guizhou. Quaternary Sciences 24, 318–324 (in Chinese).
Qin, J.M., Lin, Y.S., Zhang, M.L., Li, H.C., 2000. High resolution records of δ^{13}C and their paleoecological significance from stalagmites formed in Holocene Guilin. Quaternary Sciences 20, 351–358 (in Chinese).
Shen, C.-C., Edwards, R.L., Cheng, H., Dorale, J.A., Thomas, R.B., Moran, S.B., Weinstein, S.E., 2002. Uranium and thorium isotopic and concentration measurements by magnetic sector inductively coupled plasma mass spectrometry. Chemical Geology 185, 165–178.
Shen, C.-C., Cheng, H., Edwards, R.L., Moran, S.B., Edmonds, H.N., Hoff, J.A., Thomas, R.B., 2003. Measurement of attogram quantities of ^{231}Pa in dissolved and particulate fractions of seawater by isotope dilution thermal ionization mass spectroscopy. Analytical Chemistry 75, 1075–1079.
Shen, C.-C., Li, K.-S., Sieh, K., Natawidjaja, D., Cheng, H., Wang, X., Edwards, R.L., Lam, D.D., Hsieh, Y.-T., Fan, T.-Y., Meltzner, A.J., Taylor, F.W., Quinn, T.M., Chiang, H.-W., Kilbourne, K.H., 2008. Variation of initial ^{230}Th/^{232}Th and limits of high precision U–Th dating of shallow-water corals. Geochimica et Cosmochimica Acta 72, 4201–4223.
Wan, N.-J., Li, H.-C., Liu, Z.-Q., Yuan, D.-X., Chen, Y.-H., 2011. Spatial variations of monsoonal rain in eastern China: Instrumental, historic and speleothem records. Journal of Asia Earth Sciences 40, 1139–1150.
Wang, B., 2006. The Asian Monsoon. Springer Praxis Publishing, Chichester, UK, ISBN 3-540-40610-7, 787p.
Wang, D.L., Zhu, S.Q., Huang, B.L., 2004. Discussion on the conception and connotation of rocky desertification. Journal of Nanjing Forestry University (Natural Science Edition) 11, 87–90 (in Chinese).
Wang, Y.J., Cheng, H., Edwards, R.L., He, Y.Q., Kong, X.G., An, Z.S., Wu, J.Y., Kelly, M.J., Dykoski, C.A., Li, X.D., 2005. The Holocene Asian monsoon: links to solar changes and North Atlantic climate. Science 308, 854–857.
Wang, Y.J., Cheng, H., Edwards, R.L., An, Z.S., Wu, J.Y., Shen, C.-C., Dorale, J.A., 2001. A high-resolution absolute-dated late Pleistocene monsoon record from Hulu Cave, China. Science 294, 2345–2348.
Xiong, K.N., Li, P., Zhou, Z.F., 2002. Study of GIS on Karst Desertification. Geological Press, Beijing. pp. 1–183 (in Chinese).
Yuan, D.X., Cheng, H., Edwards, R.L., Dykoski, C.A., Kelly, M.J., Zhang, M.L., Qing, J.M., Lin, Y.S., Wang, Y.J., Wu, J.Y., Dorale, J.A., An, Z.S., Cai, Y.J., 2004. Timing, duration, and transitions of the last interglacial Asian monsoon. Science 304, 575–578.
Zhang, D.E., Li, X.Q., Liang, Y.Y., 2003a. Continuation (1992–2000) of the Yearly Charts of Dryness/Wetness in China for the Last 500 years period. Journal of Applied Meteorological Science 14, 379–388 (in Chinese).
Zhang, D.E., Li, H.-C., Ku, T.-L., Lu, L.H., 2010. On linking climate to Chinese dynastic change: spatial and temporal variations of monsoonal rain. Chinese Science Bulletin 55, 77–83.
Zhang, M.L., Lin, Y.S., Qin, J.M., Cheng, H., 2002. The record of paleoclimatic change from stalagmites and the determination of termination II in the south of Guizhou Province, China. Science in China 32, 942–950 (in Chinese).
Zhang, M.L., Lin, Y.S., Qin, J.M., Zhang, C., Tu, L.L., Cheng, H., 2003b. The record of paleoclimatic change and the termination of the last interglacial period from a stalagmite of Qingxin Cave in south Guizhou. Acta Sedimentologica Sinica 21, 473–481 (in Chinese).
Zhao, C., Wang, Z.R., Tao, K., Wang, J.H., Lin, Y.S., Zhang, M.L., 2004. Reconstruction of the paleoclimate and paleoenvironment of a stalagmite from Longquan cave, Guizhou between 1600–250 a. Chinese Journal of Nature 26, 209–214 (in Chinese).